

Sulfide driven fuel cell performance enhanced by integrated chemisorption and electricity generation

S. Stefanov¹, D. Uzun², L. Ljutzkanov¹, V. Beschkov^{1*}

¹*Institute of Chemical Engineering, Bulgarian Academy of Sciences, 1113 Sofia, Bulgaria*

²*Institute of Electrochemistry and Energy Systems, Bulgarian Academy of Sciences, 1113 Sofia, Bulgaria*

Received: May 23, 2024; Revised: July 14, 2024

This study is related to the direct utilization of the hydrogen sulfide in the Black Sea water as energy source in a sulfide-driven fuel cell. One of the main obstacles for the practical application of this process is the low concentration of hydrogen sulfide, less than 20 g dm⁻³.

We propose a scheme of preliminary saturation with sulfide from the sea water of an electro-conductive sorbent doped by metal oxides, forming sulfides with low solubility. The latter simultaneously serve as sorbent and electrode (anode). The next step is sulfide oxidation at a regime of fuel cell with generation of electromotive force. The resulting oxidation products are removed by elution with a solution of supporting electrolyte. We achieved two goals: first, concentration of sulfide on the sorbent to practically significant amounts and second, electricity production in a fuel cell mode together will sorbent regeneration.

Our experiments were carried out in a membraneless fuel cell with gas-diffusion electrode as cathode containing a catalyst doped with compounds of cobalt and manganese. The anode was doped by zinc oxide embedded into electro-conductive char produced by pyrolysis of waste soot. The sorption capacity of the sorbent was practically independent on the sulfide concentration in the feeding solution.

The experimental results show the stable work of both electrodes with high sorption capacity for sulfide on the anode (0.15%wt.), high current density (up to 20 A/m²) and power density (up to 2.5 W/m²). Different products of sulfide oxidation were detected, namely, polysulfide, sulfite and sulfate. Polysulfides were detected when the sulfide concentrations in the eluting solution were rather high. The oxidation products at low sulfide concentrations are mainly sulfite and sulfate.

Keywords: sulfide fuel cell, chemo-sorption, catalysis, gas diffusion electrode

INTRODUCTION

The present paper deals with the use of sulfide as a fuel for sulfide-driven fuel cell. Cases were considered when the sulfide concentration is low and its direct feed in the fuel cell is not practically reliable.

It is the case of the Black Sea where the amount of hydrogen sulfide is enormous, but its concentration is rather low, i.e. it reaches up to 20 g m⁻³ at the biggest depth (*ca.* 2200 m) [1, 2]. This fact makes the use of hydrogen sulfide not suitable as a fuel for practical purposes. There is an effort for stripping of hydrogen sulfide from marine water by heating and further processing in gaseous phase [3, 4]. This process is accompanied by considerable input of thermal energy.

There are some other efforts, each of them associated to the separation of hydrogen sulfide by membrane processes [5], membrane separation with consequent pressure swing adsorption in gaseous phase [6]. Dutta *et al.* have proposed a sulfide driven fuel cell operating in gaseous phase [7]. The drawback in this case is the released sulfur being

harmful for the anodes. Kim & Han [8] have studied a liquid phase sulfide fuel cell attaining high current densities but in very strong alkaline medium, i.e. 3N NaOH, which is harmful for the marine aquatic life.

In the last decade some of the authors of the present paper proposed the use of sulfide-driven fuel cell in aqueous solutions to produce electricity and clean the sea water to some extent [9, 10]

In our case the goal is to increase the sulfide concentration in the aqueous phase to reach practically important current and power densities during sulfide-driven fuel cell operation. One possible way to overcome the drawback of low sulfide concentrations in the feed is to adsorb sulfide anions on ion-exchange resin and then to elute sulfide by a certain eluent (e.g. sodium hydroxide solution) with desired amount and flow rate to increase sulfide concentration to an appropriate level. There are attempts for sulfide retention on anion-exchange resins [11, 12], but the problem is the difficult back-elution of sulfide. Another problem is the use of more alkaline eluent (like sodium hydroxide) which is not appropriate from environmental point of view.

* To whom all correspondence should be sent:
E-mail: vbeschkov@yahoo.com

Our idea is to compose a electro-conductive chemo-sorbent which absorbs sulfides as chemical compounds, like metal sulfides [13]. This sorbent also serves as anode in the fuel cell.

First, sulfide react with metal oxide embedded into electro-conductive carbon matrix to form metal sulfide.

The second step is elution in a fuel cell mode by the initial sulfide solution or by a supporting electrolyte. Thus, the formed metal sulfides are directly oxidized on the anode, the oxidation products are removed, and the sorption activity of the chemo-sorbent is restored. Thus, electromotive force is generated.

Using this approach, the amount of the captured sulfide depends on the amount of the active metal oxide in the matrix. So, one can regulate the fuel cell capacity according to the required power density.

On the other hand, we decided to use a gas-diffusion cathode with appropriate catalyst to enhance oxygen reduction, to avoid the adverse effect of the low oxygen solubility in aqueous solutions and the mass transfer limitations.

The gas-diffusion electrode (GDE) is a porous electrode where the solid catalyst is in contact with both liquid electrolyte and gas phase, as described in the literature [14-16].

GDEs have a structure that mainly consists of a super-hydrophobic layer (gas phase layer), a gas diffusion layer (solid phase layer) and a catalytic layer (liquid phase layer). The gas is transported to the catalytic bed through the gas diffusion bed [17]. At the same time, the gas diffusion layer prevents the gas diffusion channel from being covered due to electrolyte migration [18]. GDEs are naturally assumed to possess the properties of air permeability and hydrophobicity. Therefore, oxygen/air transport in the gas phase layer plays an important role in sulfate production [19]. The main function of the gas diffusion layer is to collect electrons, facilitating gas transport and chemical reactions, i.e. oxygen reduction in this case. The catalyst is supported on the surface of the catalytic layer, where oxygen can be reduced due to its hydrophilicity under the action of catalyst (solid phase) and electrolyte (liquid phase) [16].

There are some attempts to use gas-diffusion electrodes (GDE) for sulfite oxidation [20] and sulfide oxidation in liquid phase anode fuel cells [21, 22] showing good performance.

Therefore, a membraneless fuel cell was selected with a specially designed gas-diffusion cathode

containing cobalt and manganese compounds as catalyst.

The aim of this study is to demonstrate the combination of integrated preconcentration of sulfide on the anode serving also as sorbent and consequent electricity production in a liquid phase fuel cell with gas-diffusion cathode.

MATERIALS AND METHODS

Materials

Experiments with a sorbent used as anode were carried out. The sulfide solutions were prepared by sodium sulfide nona-hydrate ACS reagent $\geq 98\%$ purity (Sigma-Aldrich production). All other chemicals used for analyses were of p.a. grade.

A sodium chloride solution in distilled water was used as a supporting electrolyte for the anodic compartment. The chosen sodium chloride concentration corresponds to the Black Sea water, i.e., 16 g dm^{-3} . The pH of the initial solution varied between 7.3 and 12.6 depending on the chosen sulfide concentration from 20 to 1200 mg dm^{-3} .

The catalyst for the cathode was embedded in the gas-diffusion electrode (GDE). The catalyst consisted of oxides of manganese and cobalt, i.e. $\text{MnCo}_2\text{O}_{4.5}$. It was prepared by pyrolysis of ground apricot stones, soaked in acetates of the listed metals. The gas-diffusion electrode (GDE) was prepared in a way close to the method previously developed at the Institute of Electrochemistry and Energy Systems at the Bulgarian Academy of Sciences, described in [14] and later using Vulcan XC-72 R [10]. GDE consists of two layers - a gas-diffusion layer of 50 mg cm^{-2} of teflonized Vulcan XC-72 R (35 % Teflon) and an active layer of 50 mg cm^{-2} of $\text{MnCo}_2\text{O}_{4.5}$ mixed with 15 mg cm^{-2} of Vulcan XC-72 R. Cobalt in combination with manganese in the resulting electrocatalytic mass plays an important role in the diffusion process. There is no evidence of decomposition of the carbon residue and/or passage of Co into solution. GDE works quite efficiently in both alkaline and neutral electrolytes.

The cathode area was 12.5 cm^2 . The XRD-diagram of the catalyst is shown in Fig. 1. It consists of 47% MnO (manganosite) and 53% cobalt.

The chemo-sorbent was prepared by pyrolysis of waste soot from tire production, soaked in zinc acetate. Its XRD-diagram is shown in Fig. 2. The sorbent particles were of 0.1 μm average size. The prepared chemo-sorbent is electro-conductive and thus it enlarges the apparent anode area.

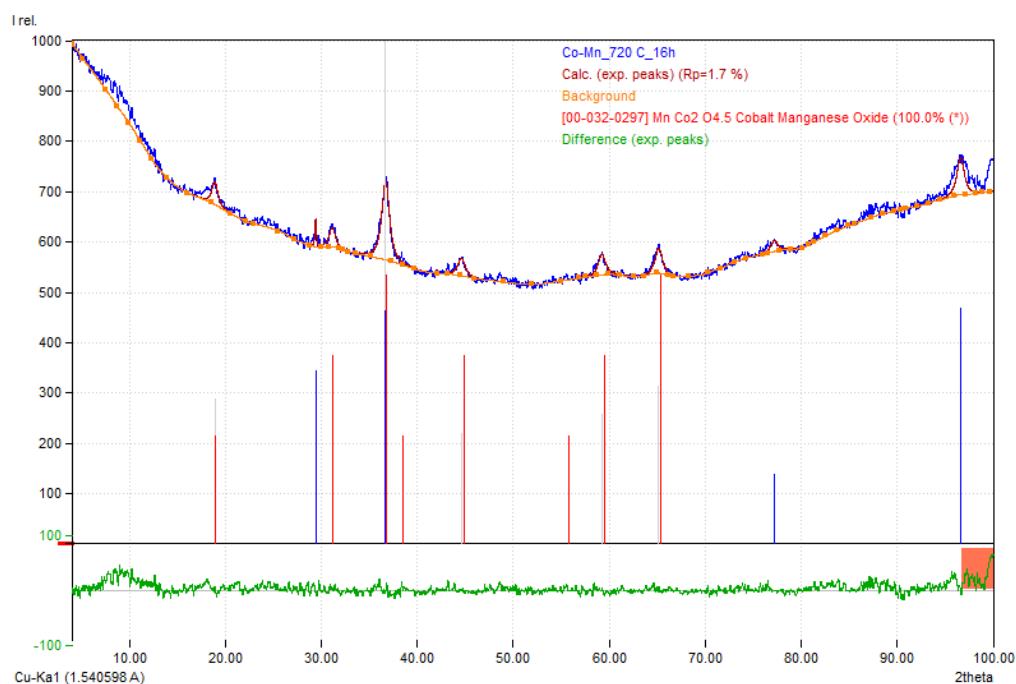


Figure 1. XRD-diagram of the prepared and used catalyst for cathode application.

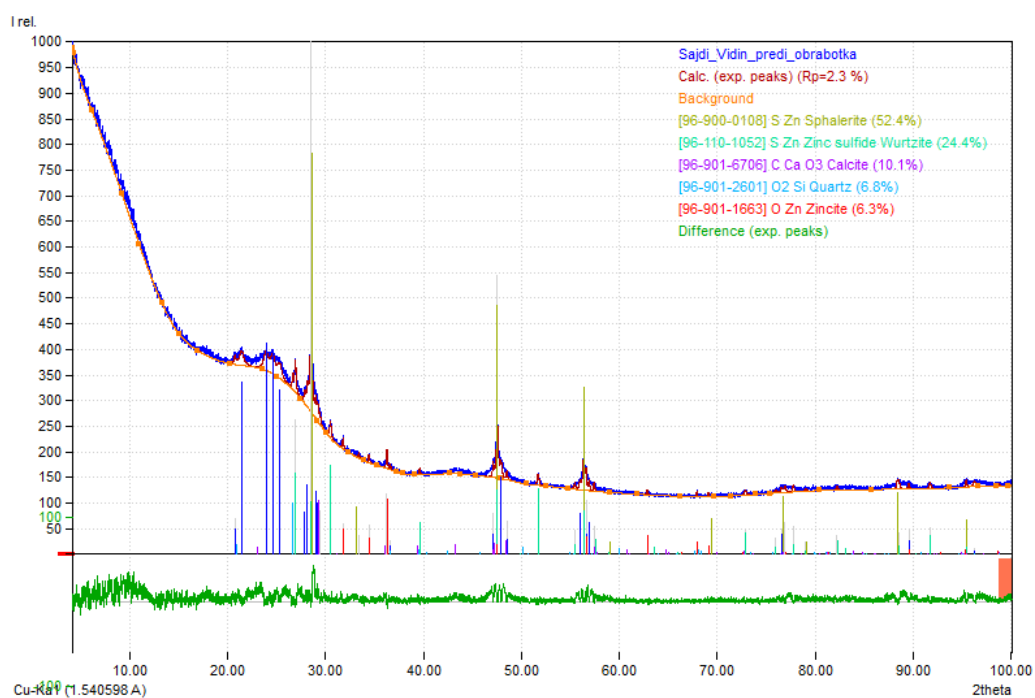
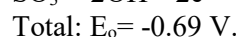
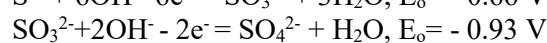
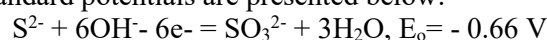


Figure 2. XRD-diagram of the prepared and used as anode chemo-sorbent containing zinc oxide and sulfide.

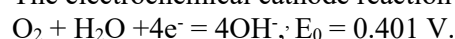
Experimental design

The fuel cell consisted of a rectangular compartment of 370 cm³ volume. The external gas diffusion electrode was mounted at one of the walls with access to the air outside. The anode compartment was packed with the sorbent. Graphite rods were used as contact anodes. Continuous processes for the anode compartment were studied with a feed flow rate of 0.300 dm³ h⁻¹.

The expected scheme of the fuel cell for the considered case is shown in Fig. 3. The anode reactions of consecutive sulfide to sulfate oxidation involving hydroxylic anion exchange with their standard potentials are presented below:



The electrochemical cathode reaction is:



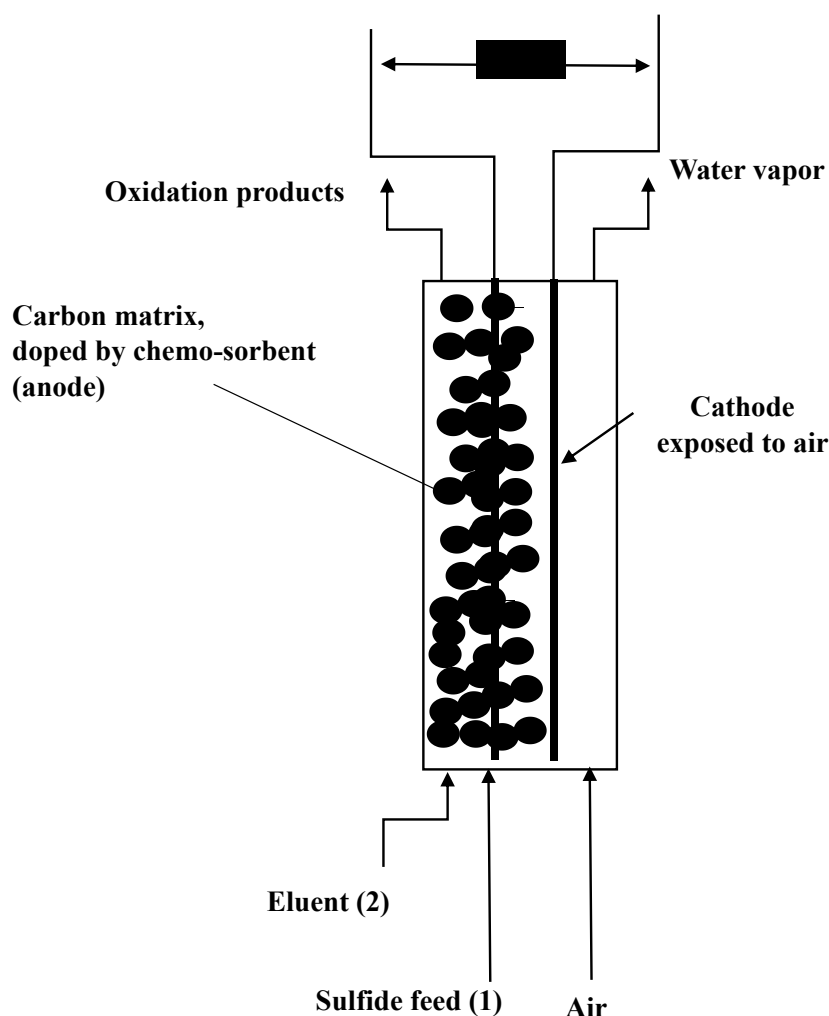


Figure 3. Scheme of the operation mode of membraneless sulfide-driven fuel cell.

Before the experiments, as a first step the chemo-sorbent in the anode compartment of the fuel cell was saturated for several hours with sulfide anions by continuous feeding with sulfide solutions of different concentrations, from 20 to 1200 mg dm⁻³. During the saturation the open circuit voltage (OCV) of the cell was monitored. Samples from the inlet and outlet solution were taken and analyzed for sulfide. The sorption capacity (wt.%) was calculated by the difference in inlet and outlet concentrations for the used flow rate. The sorption capacity was calculated as the sorbed amount of sulfide to a unit mass of the used chemo-sorbent. The saturation ended when the OCV value became practically constant. Then the sorbent was eluted in a fuel cell mode by a low-concentration solution of sulfide (ca. 20 g dm⁻³) in 16 g dm⁻³ sodium chloride solution as supporting electrolyte. Thus, electromotive force was generated together with regeneration of the chemo-sorbent by *in situ* anode oxidation of the retained sulfide. Some experiments at higher inlet concentrations of sulfide (i.e. from 200 up to 1200 mg dm⁻³) in the eluting solution were made too. The

continuous feeding was accomplished by a peristaltic pump.

During the continuous experiments the inlet sulfide solution was purged by nitrogen prior to supplying it to the fuel cell to avoid or at least to minimize the parasite bulk oxidation of sulfide.

Samples from the inlet and outlet flows were taken regularly and analyzed quantitatively for sulfide, and qualitatively for sulfite, sulfate, thiosulfate and polysulfide. Fourteen experiments were carried out both using the same gas-diffusion cathode and chemo-sorbent. After each saturation, polarization curves were taken at different current densities varying the external resistance of the circuit. Then, experiments on the cell discharge through selected ohmic resistance by continuous feed by sulfide solutions were carried out. The electric current values were calculated by the Ohm's law from the measured cell voltage and the external resistance.

The amounts of oxidized sulfide were calculated from the evaluated electric current according to the Faraday's law and compared to the converted sulfide according to the analyses.

$$\frac{m}{t} = \frac{M_i}{nF}, m = \frac{M}{nF} \int_0^t i. dt \quad (1)$$

where: i —electric current, A; m —mass of reacting substance, g; t —time, s; M —molar mass of reacting substance, g; n —number of exchanged electrons; F Faraday constant = 96,484 C mol⁻¹.

The number of exchanged electrons n depends on the reactions on the anode. In the case of sulfide oxidation these reactions are very sensitive to the sulfide concentration and a large variety of exchanged electrons for different electrochemical reactions are possible. We shall constraint ourselves to some of them which are more probable at lower sulfide concentrations, as in our case. Table 1, excerpt of a comprehensive one [23] is shown below.

Table 1. Short excerpt of sulfide oxidation reactions, taken from [23]

No.	Reversible anode reaction	Number of exchanged electrons, n	Standard electrode potential, V, 25°C
1	$\text{SO}_4^{2-} + \text{H}_2\text{O} + 2\text{e} = \text{SO}_3^{2-} + 2\text{OH}^-$	2	-0.91
2	$\text{SO}_3^{2-} + 3\text{H}_2\text{O} + 6\text{e} = \text{S}^{2-} + 6\text{OH}^-$	6	-0.66
3	$\text{S}_2^{2-} + 2\text{e} = 2\text{S}^{2-}$	1	-0.524
4	$\text{S}_3^{2-} + 2\text{e} = \text{S}^{2-} + \text{S}_2^{2-}$	1	-0.49
5	$\text{S} + 2\text{e} = \text{S}^{2-}$	2	-0.48
6	$\text{S}_2\text{O}_3^{2-} + 6\text{H}^+ + 8\text{e} = 2\text{S}^{2-} + 3\text{H}_2\text{O}$	4	-0.006

Table 2. Comparison of the oxidized amount of sulfide according to the current yields to that determined by analyses of the inlet and outlet flows at different inlet concentrations of sulfide. Elution flow rate 0.3 dm³ h⁻¹.

Run No.	Inlet concentration, mg dm ⁻³	Amount of oxidized sulfide, mg 1 exchanged electron	Amount of oxidized sulfide, mg 2 exchanged electrons	Amount of oxidized sulfide, mg 8 exchanged electrons	Amount of oxidized sulfide, analysis, mg	Oxidized forms found in the outlet flow
1	239.7	8.92	4.96	1.12	14.01	Polysulfide, sulfite, sulfate
2	24.9	15.0	7.5	1.88	8.96	Sulfite
3	23.5	16.7	8.35	2.09	5.88	Sulfite
4	1195	41.01	20.5	5.13	501.85	Polysulfide, sulfite, sulfate
5	24.7	16.8	8.4	2.1	13.4	Sulfite, sulfate
6	21.8	5.28	2.64	0.66	7.96	Sulfite, sulfate
7	19.5	6.24	3.12	0.78	6.64	Sulfite, sulfate

Analyses

Sulfide was analyzed photometrically with N,N-dimethyl-*p*-phenylenediamine in the presence of Fe(III) to form methylene blue [24]. Sulfate and sulfite were qualitatively proven by the addition of barium chloride. Barium sulfite is soluble in acid medium whereas barium sulfate is not. The presence of thiosulfate was checked by the addition of ferric salts leading to purple color. Polysulfides give a colored clear solution (yellow for S₂²⁻ and green for S₃²⁻) with deposition of sulfur in acid medium.

During all experiments the acidity of the inlet and outlet flows was monitored by measuring the pH. A glass electrode coupled with a Seven easy pH-meter (Mettler Toledo) was used.

RESULTS AND DISCUSSION

Chemo-sorption capacity

The summarized results for the oxidized sulfide calculated by the Faraday's law for different anode reactions compared to the results of the chemical analysis are shown in Table 2. There, the detected products of sulfide oxidation are presented too.

The results for the sorption capacity and the limit open circuit potential of the fuel cell are shown in Fig. 4. It is obvious that both quantities are stable at continuous use for long period of time (i.e. about three months and 14 experiments).

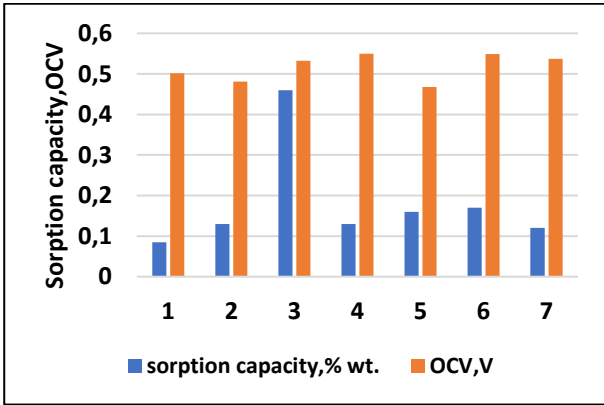


Figure 4. Sorption capacities and open circuit voltage during saturation of chemo-sorbent by sulfide at different concentrations.

Except for run 3, all sorption capacities are of the same order of magnitude, i.e. 0.16 ± 0.04 wt.%. The open circuit voltage at saturation negligibly differs depending on the concentration of saturation. Its average value is 0.54 ± 0.02 V.

An attempt was made to find a correlation between the concentration of saturation and the sorption capacity and/or the open circuit voltage, OCV. For the sorption capacity the correlation coefficient was 0.03, whereas for the open circuit voltage it was 0.0001. It means that both are practically independent of the concentration of saturation and chemo-sorption practically occurs.

A kinetic curve for the OCV variation during sorbent saturation is shown in Fig. 5.

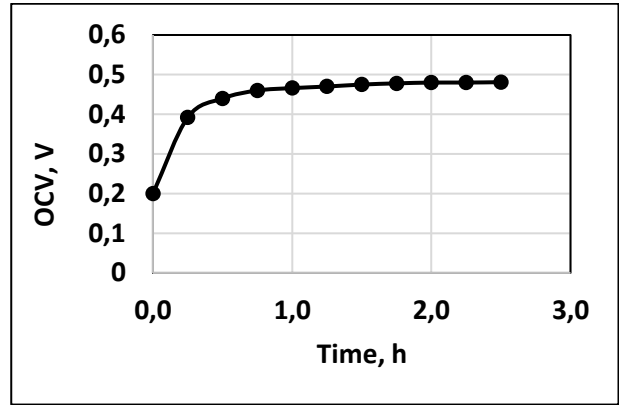


Figure 5. Variation of open circuit voltage (OCV) during saturation with sulfide (run 2). Sulfide concentration of saturation 230 mg dm^{-3} . Flow rate $0.3 \text{ dm}^3/\text{h}$.

Fuel cell performance

A polarization curve for continuous feed, obtained after preliminary saturation by sulfide for one experiment, is shown in Fig. 6.

There is a strictly linear dependence between the current density and the cell voltage with a negligible overpotential (about 1 mV) and practically no mass transfer effects at higher current densities.

The results for the cell discharge through external resistance of 10Ω for the same experiment (run 2, Table 2) are shown in Figs 7 a, b. It is evident that after a transient process in the beginning all measured quantities remain constant and stable for 4 hours. The same effect was observed for all experiments, no matter of the feeding concentration of sulfide.

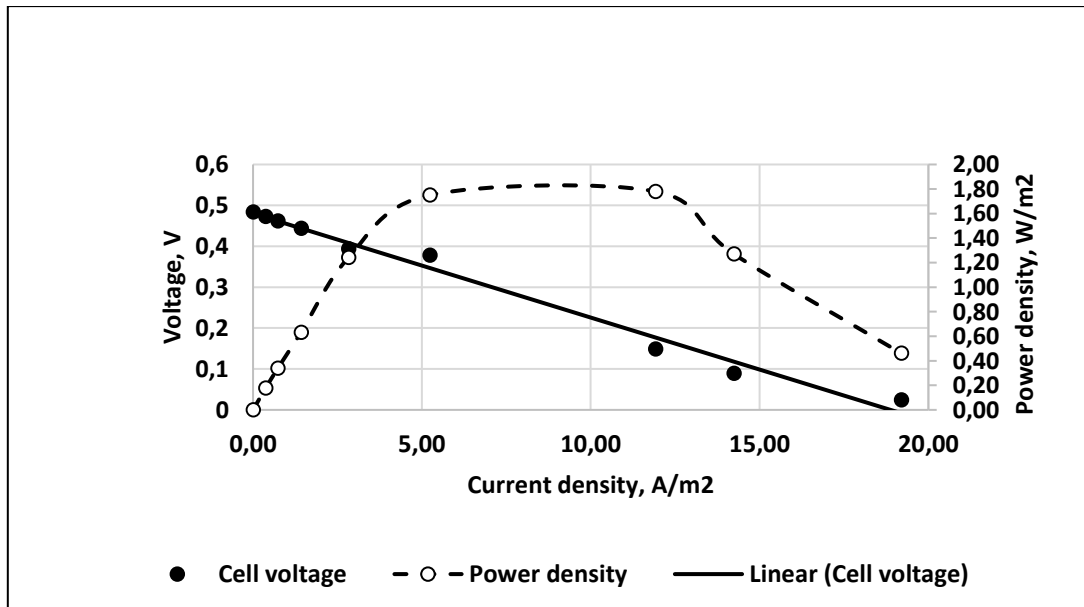


Figure 6. Polarization curve for run 2 after saturation. Sulfide concentration 24.9 mg dm^{-3} . Continuous process. Flow rate $0.3 \text{ dm}^3/\text{h}$.

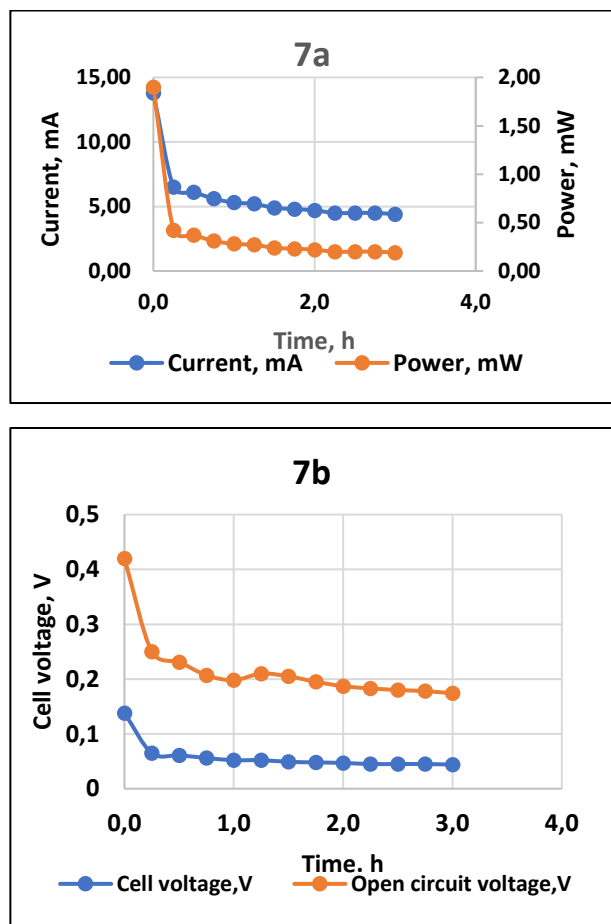


Figure 7. Discharge curves for run 2. Sulfide concentration 24.9 g dm^{-3} . Continuous process. Flow rate $0.3 \text{ dm}^3/\text{h}$. External ohmic resistance 10Ω . 7a – curves for electric current and power generated in the fuel cell. 7b – open circuit voltage (OCV) and cell tension during the discharge experiment.

The calculated depleted amounts of sulfide from the current yields according to the Faraday law for each experiment are compared to the amounts determined from the analyses of the inlet and outlet sulfide concentrations, *cf.* Table 2.

There are experiments (runs 1, 4) where the calculated amounts for oxidized sulfide by the Faraday's law are much less than those determined by analysis. This fact can be explained in the cases of high inlet concentrations of sulfide by parallel parasite reactions in the bulk and by polysulfide formation through competitive anode reactions at excessive amounts of sulfide, e.g. rows 3 and 4 in Table 1. An indication for this conclusion is the polysulfide detected in the outlet flow. Next, too large apparent amounts of depleted sulfide at high inlet concentrations are determined by analyses in the outlet flow, compared to those calculated from the current efficiency, *cf.* rows 1 and 4, Table 2. For those cases the calculated amounts according to the

Faraday's law correspond to numbers of exchanged electrons less than unity. However, one must keep in mind that many competitive reactions of sulfide oxidation may occur on the anode at high sulfide concentration. On the other hand, neither thiosulfate nor elemental sulfur were detected in the outlet stream.

In the cases of low sulfide feed concentration, the electrochemical oxidation of sulfide to sulfite and sulfate prevails, *cf.* rows 2, 3, 5-7, Table 2. Electrochemical reactions involving exchange of two electrons are sulfide-to-sulfur oxidation and sulfite to sulfate oxidation, *cf.* Table 1, rows 1 and 5. However, no sulfur was detected in the outlet flows. Therefore, it is likely to expect partial oxidation of sulfide to sulfite in the bulk with a subsequent full electrochemical oxidation to sulfate on the anode, reactions 1 and 2 in Table 1. The comparison of the oxidized amounts of sulfite to sulfate on the anode to those determined by analysis shows fuel cell efficiency from 33% (run 6) to 83.7% (run 2) if electrochemical reaction (1) in Table 1 is assumed. The direct electrochemical oxidation of sulfide to sulfate, involving exchange of 8 electrons is not likely. Probably, it takes place in a two-step consecutive scheme, *cf.* reactions 2 and 1 in Table 1.

Current and power densities

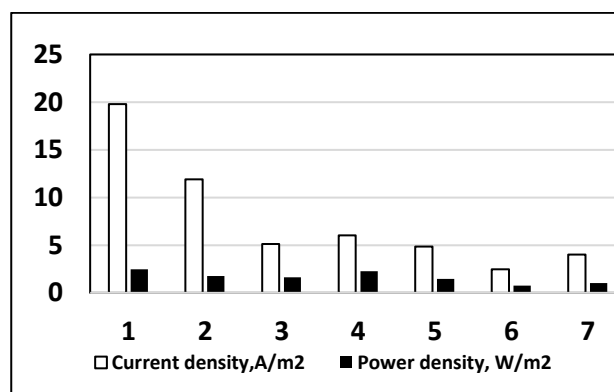


Figure 8. The maximum power and the corresponding current density for the runs presented in Table 1.

The maximum power and the corresponding current densities were determined from the polarization curves for each experiment. They are shown in Fig. 8. The highest current density, i.e. 19 A/m^2 was observed in the first experiment (run 1). The current density diminishes with the consecutive runs reaching almost stable value (4.5 A/m^2) after the third run, not depending on the inlet sulfide concentration. This decrease can be explained by some wash-out of the active component of the sorbent, i.e. ZnS in the freshly prepared sorbent. This conclusion was confirmed by XRD analyses of the sorbent prior to and after five experiments, *cf.* Table

3. It is seen that wurtzite is considerably removed after five runs and there is a slight decrease in the content of zincite.

Table 3. Percentage shares of the components in the anode chemo-sorbent before and after five runs by XRD-analyses.

Component	Before experiments, content %	After five runs, content %
ZnS, sphalerite	52.4	53.1
ZnS, wurtzite	24.4	16.6
CaCO ₃	10.1	10.3
SiO ₂	6.8	15.0
ZnO, zincite	6.3	5.06

The situation for the maximum power densities is similar. It starts with a value of 2.46 W/m² for the first run and slowly decreases to about 1 W/m² for the last two runs.

The comparison with the available data in the literature shows somewhat lower results than those reported by Wei *et al.* [20]. They measured current and power densities of 60 A/m² and 6 W/m² in a sulfite/air fuel cell. Wei & Wu [21] presented results for sulfide/air fuel cell with maximum current density of 200 A/m² and maximum power density of 9 W/m². In this study elemental sulfur was produced. In another study [22] current density of 65 A/m² and power density of 2.6 W/m² were reported. The difference can be sought in the fuel cell design and the used catalyst in the GDE. In [22] a silver catalyst directly synthesized on the cathode has been used whereas in [20] a Pt-Pd catalyst has been tested.

CONCLUSIONS

From the obtained results the following conclusions can be drawn:

1. Consecutive chemo-sorption of sulfide and elution with simultaneous anode oxidation with electromotive force generation are proposed as a method for enrichment of low-concentration sulfide solutions. The method is demonstrated in a sulfide-driven fuel cell. The anode is composed of electro-conductive carbon particles doped by zinc oxide, serving as sorbent and catalyst.

2. Gas diffusion electrode doped by cobalt and manganese compounds is successfully used as cathode in order to eliminate the mass transfer limitations and the low solubility of oxygen in aqueous solutions.

3. The electrodes show good stability after fourteen consecutive runs. The sorption capacity remains stable and practically independent of the concentration of sulfide in the saturation solution.

4. The fuel cell parameters (current and power densities) are stable for the whole set of experiments

and of the same order of magnitude as some data in the literature for fuel cell performance with sulfite and sulfide as a fuel.

5. The anode processes are sensitive to the sulfide concentration in the feeding solution. Sulfite and sulfate are the oxidation products at low sulfide concentrations. At higher concentrations in the feed polysulfide are formed because of competitive anode reactions at excess of sulfide and due to bulk reactions.

Acknowledgement: This work was supported by the Fund for Scientific Research, Bulgaria, Project KP-06-H67/3.

REFERENCES

1. A. Midilli, M. Aya, A. Kale T. N. Veziroglu, *Int. J. Hydrogen Energy*, **32**, 117 (2007).
2. I. I. Volkov, L. N. Neretin. Hydrogen Sulfide in the Black Sea, in: A. G. Kostianoy, A. N. Kosarev, (eds) *The Black Sea Environment. The Handbook of Environmental Chemistry*, vol. 5Q, Springer, Berlin, Heidelberg, 2007. https://doi.org/10.1007/698_5_083
3. N. A. Azarenkov, B. V. Borts, V. I. Tkachenko, *East Eur. J. Phys.*, **1**, 4 (2014).
4. S. A. Naman, I. E. Ture, T. N. Veziroglu, *Int. J. Hydrogen Energy*, **33**, 6577 (2008).
5. S. Gunes-Durak, S. Kapkin, *Int. J. Hydrogen Energy*, **50**, 706 (2024). <https://doi.org/10.1016/j.ijhydene.2023.11.141>
6. R. Simova, R. Velichkova, M. Uzunova, R. Angelova, P. Stankov, K. Atanasov, *Polityka Energetyczna – Energy Policy Journal*, **26**, 183 (2023). doi: 10.33223/epj/163372
7. P. K. Dutta, K. Rabaey, Z. Yuan, J. Keller, *Water Res.*, **42**, 4965 (2008)
8. K. Kim, J.-I. Han, *Int. J. Hydrogen Energy*, **39**, 7142 (2014).
9. V. Beschkov, E. Razkazova-Velkova, M. Martinov, S. Stefanov, *Appl. Sci.*, **8** (10), 1926 (2018). doi:10.3390/app8101926.
10. D. Uzun, E. Razkazova-Velkova, K. Petrov, V. Beschkov, *Bulg. Chem. Commun.*, **47**, 859 (2015). doi:10.1088/1742-6596/2710/1/012034.
11. C. Romero Cotrino, Control of Hydrogen Sulfide from Groundwater Using Packed-Bed Anion Exchange and Other Technologies, Master's Thesis, University of South Florida, Tampa, FL, USA, 2006, p. 8.
12. C. Romero Cotrino, A. D. Levine, P. Amitzoglou, J. S. Perone, *Florida Water Resources J.*, November, 22 (2007).
13. L. Ljutzkanov, V. Beschkov, S. Stefanov, E. Razkazova-Velkova, Method for electrical energy production from aqueous solutions containing hydrogen sulfide and/or sulfide, Application for BG patent, reg. No.BG/P/2022/113529.

14. I. Iliev, J. Mrha, S. Gamburgzev, A. Kaisheva, *J. Power Sources*, **17**, 345 (1986).
15. J. Xi, J. Jing, J. Gu, J. Guo, Y. Li, M. Zhou, *J. Environ. Chem. Eng.* **10**, 107882 (2022). doi.org/10.1016/j.jece.2022.107882
16. M. Zhu, H. Ge, X. Xu, Q. Wang, *Heliyon*, **4**, E00729 (2018). <https://doi.org/10.1016/j.heliyon.2018.e00729>].
17. E. Murawski, N. Kananizadeh, S. Lindsay, A. M. Rao, S. C. Papat, *J. Power Sources*, **481**, 228992 (2021).
18. K. U. Hansen, F. Jiao, *Joule* **5**, 754 (2021) doi: 10.1016/j.joule.2021.02.005
19. J. Uzun, E. Razkazova–Velkova, K. Petrov, V. Beschkov, *J. Appl. Electrochem.*, **46**, 943 (2016) doi: 10.1007/s10800-016-0979-4.
20. J. Wei, Y. Gu, X. Wu, *Sustainable Energy Fuels*, **5**, 3666 (2021). doi: 10.1039/D1SE00659B
21. J. Wei, X. Wu, *ACS Environ. Sci. Technol. Water*, **3**, 3428 (10) (2023). <https://doi.org/10.1021/acsestwater.3c00436>. 2023
22. J. Wei, Y. Liu, X. Wu, *Separ. Purif. Technol.*, **329**, 125234 (2024).
23. A.M. Suhotin, Guidebook on Electrochemistry, Himia, Leningrad, Russia, 1981 (in Russian).
24. E. Rees, T. D. Gyllenpetz, A. B. Docherty, *Analyst*, **96**, 201 (1971).